Iranian Journal of Hydrogen & Fuel Cell 1(2017) 13-26

Iranian Journal of Hydrogen & Fuel Cell

IJHFC

Journal homepage://ijhfc.irost.ir

Investigation of carbon dioxide capture from hydrogen using the thermal pressure swing adsorption process: Central composite design modeling

Ali Saberimoghaddam[1,*], Vahid Khebri[2]

[1]**Department of Chemistry and Chemical Engineering, Malek Ashtar University of Technology**
[2] **Department of Chemistry and Chemical Engineering, Malek Ashtar University of Technology**

Article Information

Article History:

Received:
03 May 2017
Received in revised form:
10 July 2017
Accepted:
15 July 2017

Keywords

Response surface methodology
Pressure Swing Adsorption
CO_2 capture
Zeolite 5A
Hydrogen purification

Abstract

In this study pre-combustion capture of carbon dioxide from hydrogen was performed using a 5A zeolite adsorber. A one column thermal pressure swing adsorption (TPSA) process was studied in the bulk separation of a CO_2/H_2 mixture (50:50 vol%). The adsorption dynamics of the zeolite bed were investigated by breakthrough experiments to select the suitable range for operational factors in the design of experiments. Combined effect of three important variables namely, adsorption time, purge to feed ratio, and regeneration temperature on hydrogen purity, recovery and productivity were investigated in the TPSA process using Response Surface Methodology (RSM). Predicted models show an interaction between adsorption time and regeneration temperature in the range that the experiments were performed. Optimization of the TPSA process was performed based on the goal of responses. As hydrogen purity has the large impact with respect to hydrogen recovery and productivity in industry, the optimum condition was proposed based on maximum purity of hydrogen. In this condition, predicted values for adsorption time, purge to feed ratio, and regeneration temperature were 7.99 min, 0.2, and 204 °C, respectively. Predicted values of responses for hydrogen purity, recovery, and productivity were 99.88%, 50.71%, and 1.32 $\frac{L}{s.gr}$, respectively. Acquired models were validated by experimental data in predicted conditions and actual responses were very close to predicted values. These results confirmed the accuracy of obtained models.

1. Introduction

The emission of gaseous products of combustion, mainly carbon dioxide, to the atmosphere is regarded as a major cause of global warming and climate change through the so-called greenhouse effect [1]. Currently, 85 % of total world energy demand is supplied by thermal power plants fed by fossil fuels,

*Corresponding Author's Fax: +982122962257
E-mail address: Articlemut@gmail.com

doi:10.22104/ijhfc.2017.2161.1135

including coal, oil and gas. They account for about 40 % of total CO_2 emissions [2]. Hydrogen is an environmentally cleaner source of energy, and it is considered as one of the most promising future energy carriers and transportation fuel. Hydrogen is known as the cleanest fuel and its reaction with oxygen produces water vapor [3, 4]. Hydrogen is not available in free molecular form on earth but can be produced using a large variety of feed stocks such as liquid and gaseous hydrocarbons or water. Natural gas steam reforming is one of the most economical routes to produce hydrogen [5]. However, the natural gas steam reformer produces hydrogen with several impurities (syngas) such as water vapor, carbon dioxide, methane, carbon monoxide and, in some cases, nitrogen [6]. The CO composition in syngas reacts with steam to generate CO_2 and H_2 via the water-gas-shift reaction. Thus, crude hydrogen stream from a steam reformer contains a significant quantity of carbon dioxide (typically 15–25%) [7] that should be removed in another process. Many processes have been used to separate carbon dioxide from the syngas mixture such as cryogenic separation, absorption in chilled methanol or ethylene glycol. These processes are energy intensive due to their heat transfer requirements, so they would likely to be replaced if higher performance and less costly technologies are demonstrated [8, 9]. Novel approaches to achieve a higher level of CO_2 capture than conventional technologies at lower capital and operating costs include adsorption with solid sorbents. High CO_2 selectivity and adsorption capacity are key properties of an adsorbent material for the separation of CO_2 from pre-combustion gas, i.e., CO_2/H_2 gas mixtures. In addition, the success of the CO_2 capture process depends on the cost and regeneration condition of the adsorbent [10, 11]. Zeolites have shown good results in CO_2 capture processes and can be used for separation of CO_2 from gas mixtures. They are inexpensive and use of these adsorbents is economical. Regeneration or reactivation of the adsor ent aims to restore the adsorption capacity of the exhaustd adsorbent for recycle as well as to recovr valuable components present in the adsorbed phase. Since adsorption operations are cyclic, the efficiency and cost of regeneration play important roles in the overall feasibility of the process [12].

The pressure swing adsorption (PSA) process is available for the regeneration of spent adsorbents: The PSA process is based on preferential adsorption of an adsorption material towards one or more components from a mixture at high pressure, and recovery of the gas at low pressure [13]. Thus, the porous sorbent can be reused for subsequent adsorption. The low recovery rate of CO_2 is one of the problems reported with zeolites in the PSA process [12]. Therefore, new methods to modify the process in order to meet the requirements of pre-combustion CO_2 capture need to be developed and implemented. To solve this problem the combination of desorption at low pressure and high temperature, which is the principle of the thermal pressure swing adsorption (TPSA) process, has been reported [10, 12, 14]. The efficiency of the TPSA process can be improved by modifying some operating parameters, such as adsorption pressure, purge-to-feed ($\frac{P}{F}$) ratio, regeneration conditions, adsorption time (Ad.t), etc. In most adsorption processes the operational factors have been optimized using the conventional one factor at a time method. In this method, one factor is varied at a time while the others are constant. So, many experiments must be performed to evaluate the interaction effect between the independent variables and finding the reliable optimum condition[15]. Statistical experimental design methods appraise the interaction of factors, requiring a much more limited number of experimental tests.

In the last few years, there has been a growing interest in the application of methods for optimization of adsorption processes . One of the statistical tools of experimental design is Response surface methodology (RSM), which can assess the effects of two or more independent variables by design of experiments and multiple regression analysis. In this method less experimental runs are needed for experiment design. This technique describes the behavior of a given set of data by fitting a polynomial

equation to the experimental data and can optimize the operational factors [16]. Recently, a few studies have been performed on the use of RSM methodology in CO_2 adsorption [14, 17]. Garcia et al. [18] studied the CO_2 equilibrium adsorption capacity and breakthrough time in a flow-through system where the adsorbent was subjected to four consecutive adsorption–desorption cycles. They used RSM to assess the combined effect of the adsorption CO_2 partial pressure and temperature on CO_2 capture capacity and breakthrough time with activated carbon as the adsorbent. Serna-Guerrero et al. [19] studied the behavior of amine-grafted mesoporous silica throughout the adsorption–desorption cycles in the presence of 5% CO_2/N_2 to determine the optimum regeneration conditions using a 2^3 factorial design of experiments. Mulgundmath and Tezel [20] compared a PSA with a TPSA process for CO_2 recovery from a flue gas composition of 10% CO_2 in N_2 using Ceca 13X adsorbent and a factorial design set of experiments. Garcia et al. [14] used the RSM methodology to assess the combined effect of three independent variables, namely, regeneration temperature, desorption pressure, and purge to feed ratio on activated carbon performance in the H_2/CO_2 separation process.

In the present work, the cyclic performance of a commercial zeolite 5A in a precombustion capture process, i.e., high CO_2 concentration, as a function of different adsorption and regeneration conditions has been evaluated by means of response surface methodology. A knowledge of adsorption/desorption dynamics in the TPSA process provide a valuable guide for design of the cyclic process. Hence, the first part of the paper focuses on the effect of feed flow rate and adsorption pressure on breakthrough behavior of a zeolite 5A bed in a H_2/CO_2 mixture to determine the best condition to perform the experiments. CO_2 desorption behavior from 5A zeolite bed was also investigated under various temperatures to assess temperature range for design of experiments using RSM. The adsorption step time, regeneration temperature (T_R), and $\frac{P}{F}$ ratio play the key roles in the development of an optimum H_2/CO_2 mixture separation process. Therefore, the efficiency of this process can be improved by modifying the operating parameters. Thus, the second part of this work deals with studying the simultaneous effects of adsorption time, purge to feed ratio, and regeneration temperature on hydrogen purity, recovery, and productivity by means of response surface methodology to model and optimize the TPSA process in the separation of a CO_2/H_2 mixture (50:50 vol%) using zeolite 5A.

2. Apparatus and procedures

A schematic diagram of the apparatus used in the TPSA process is shown in Fig. 1. The adsorption column was a stainless steel (type 304) pipe 75 cm long and 0.87 cm I.D. The column was packed with a local zeolite 5A, 20-40 mesh. Characteristics of adsorbent are shown in Table 1. To prevent the carryover of adsorbent particles, microwire mesh was placed at the ends of the bed with glass wool compressed on both side (top and bottom of the bed), an in-line filter was used to restrain entrance of fine particles to the gas lines. All lines were quarter-inch (6.4 mm) stainless steel tubes. Hydrogen (99.999%, Arad gas, Iran) and carbon dioxide (99.99%, Arad gas, Iran) were used to prepare the feed gas mixture. The gas mixture (50% CO_2 in H_2) was prepared using two MFC (mass flow controller, Alicat, USA). Check valves (CV) and microfilters were installed after the mass flow controllers to prevent reverse flow and contamination. A gas mixer (GM) was installed after the hydrogen and carbon dioxide streams for better mixing of the two gases. The gas mixture composition and the outlet gas stream from the adsorption bed was analyzed by an online gas chromatograph (TG2552, TGF Co Ltd, Iran) equipped with a gas sampling valve (10 port,VICI), a Propack Q column, a methanizer , a FID, and TCD detectors. Another MFC (3c) and a needle valve (V-06) were installed after the adsorption column to maintain constant pressure inside the adsorption bed by controlling the flow rate of the outlet stream.

Table 1. Characteristics of adsorbent

pellet size	20-40 mesh (spherical)
pellet density	1.16 g/cm^3
heat capacity	0.23 cal/g.K
Chemical composition(%)	SiO_2 (36.41), Al_2O_3 (28.14), Na_2O (10.23)

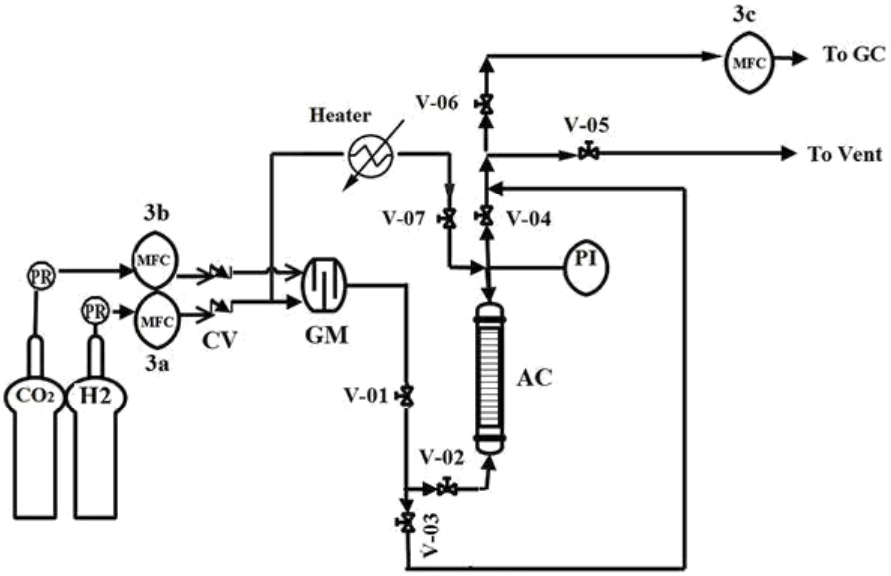

Fig. 1. Schematic diagram of apparatus for a single bed thermal pressure swing adsorption process.
PR:pressure regulator, MFC: mass flow controller, CV: check valve, GM: gas mixer, PI: pressure indicator, AC: adsorbent column.

A pressure gauge (PI) was placed at the top of the bed for reading the pressure. Needle valves were used to alternately direct the flow into and out of the column for cocurrent, contercurrent blowdown and purging. An electrical furnace was used to increase the purge gas temperature (H_2) in the purging step. Zeolite 5A was used as the adsorbent. It was activated at 300 °C for 2 h in a tubular furnace under nitrogen flow with a heating rate of 2 °C min^{-1}. After the zeolite was packed in the column and before each experiment run, the bed was purged with hot H_2 stream (210 °C) for 1 h, then, the system was pressurized to the desired pressure with a feed stream before the experiments.

2.1. TPSA process description

The TPSA cycle consisted of the following steps: (I) bed feed pressurization (PR), (II) high pressure adsorption (AD), (III) cocurrent depressurizing (CD), (IV) countercurrent depressurization blowdown (BD), (V) purge with hot hydrogen stream (PG), and (VI) cooling step. In step I, the bed was pressurized to the desired pressure by the feed stream, while V-07, V-05, and V-03 were closed; V-01,V-02, V-04, and V-06 were opened; 3a and 3b MFCs were set at desired flow rates to produce CO_2/H_2 mixture (50% vol, CO_2 in H_2); and 3c was off (no gas passed through it). The desired column pressure was controlled by the pressure regulator connected to the gas cylinder. In step (II), the high pressure gas mixture flows through the bed while 3c (MFC) was set at desired flow rates. Step (III) cocurrent blowdown, is used to recover the H_2 remaining in the voids and to allow time for CO_2 to desorb in the bed. This step was performed by closing V-01 and V-06 valves and opening V-05. Steps IV and V operate countercurrent to the feed direction, to desorbed carbon dioxide (adsorbed in step (II)) from bed and provide a cleaned bed for the next cycle. Countercurrent blowdown (step IV) was done simultaneously by closing the V-04 valve and

opening the V-03 valve. When the column pressure dropped to atmospheric pressure the 3a MFC, set at the desired flow rate, and pure hydrogen flowed through the electrical furnace increasing its temperature to the desired temperature and entered the bed through the open V-07 valve (step V). The Cooling step was done by closing the V-07 valve and decreasing the bed temperature to ambient temperature by means of a cooling device.

3. Design of the experiments

Response Surface Methodology (RSM) is one of the statistical tools of experimental design that involves multiple regression analysis and fewer experimental runs. In this study, a central composite design (CCD), as the most commonly used RSM, was carried out by Design Expert 7.0.0 software for the factors optimization. The CCD is a multivariate technique, introduced by Box and Wilson [21] as the most appropriate second order design. In this work, to design the experiments using RSM, regeneration temperature, adsorption time and purge to feed ratio were considered as the operating factors (variables) and the productivity, purity and recovery of hydrogen as the response in the experimental design. This design consists of the following parts: axial points (+α and -α), fractional factorial design points (+1 and -1), and center points. +1 and -1 levels are the boundary of modeling space. The maximum and minimum of each variable are indicated by +α and -α levels, respectively. The α value depends on the number of variables (k) and can be determined by $\alpha = 2^{k/4}$. More details about CCD design can be seen elsewhere [22-24]. The total number of required tests (N) can be determined by the following equation:

$$N = 2^k + 2k + N_0 \quad (1)$$

Where k is the number of factors and 2^k, 2k and N0 refer to the cubic, axial and the center point runs, respectively. The center point of CCD is used to calculate the experimental error.

4. Results and discussion

4.1.Preliminary experiments

Preliminary experiments were performed to determine the appropriate range of adsorption factors ($\frac{P}{F}$ ratio, Ad.t, and T_R) for design of experiments by RSM. The experiments were done to select an optimum pressure, feed flow rate, and purge gas temperature. To investigate the feed flow rate effect on breakthrough time and select the optimum feed flow rate, experiments were performed at 0.1, 0.3 and 0.5 standard liter per minute (SLPM). Fig. 2 shows the effects of feed flow rate on breakthrough curves. As can be seen in the figure, the breakthrough time decreases as the feed flow rate increases and this decrease is not linear. In other words, the difference in the breakthrough time between 0.1 and 0.3 SLPM is larger than the difference between 0.3 and 0.5 SLPM. This non-linear trend can be attributed to the mass transfer resistance which non-linearly decreases with feed flow rate increases. This phenomenon expresses that saturation of the adsorbent bed at the feed flow rate of 0.1 SLPM occurs later and there is sufficient time for evaluation of adsorption time on hydrogen purity and recovery; therefore, 0.1 SLPM was chosen as the suitable feed flow rate.

To find the proper maximum pressure, the breakthrough experiments were performed at 3, 7, and 9 bar gas feed pressures. Fig. 3 shows the breakthrough curves at 0.1 SLPM in accordance with the change in pressure. The figure shows that adsorption capacity increases at higher pressures and the breakthrough time becomes longer. However, the variation of the breakthrough time decreased slightly with an increase in adsorption pressure. In other words, this increase is not linear, for instance, pressure does not make much difference on the breakthrough time at 9 bar as compared to 7 bar. Selecting the lower pressure (7 bar) instead of 9 bar not only results in obtaining the desired product purity, but also leads to increasing the recovery. Therefore, according to the results obtained from preliminary breakthrough experiments, the cyclic TPSA experiments were carried out at 0.1 SLPM and 7 bar.

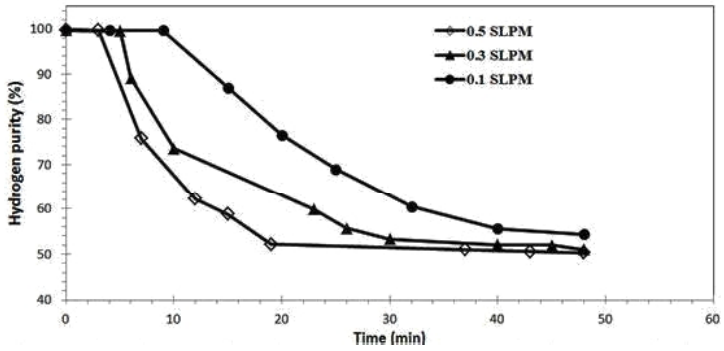

Fig.2. Effect of feed flow rate on breakthrough curves at constant adsorption pressure, 7 bar, for H_2/CO_2 mixture.

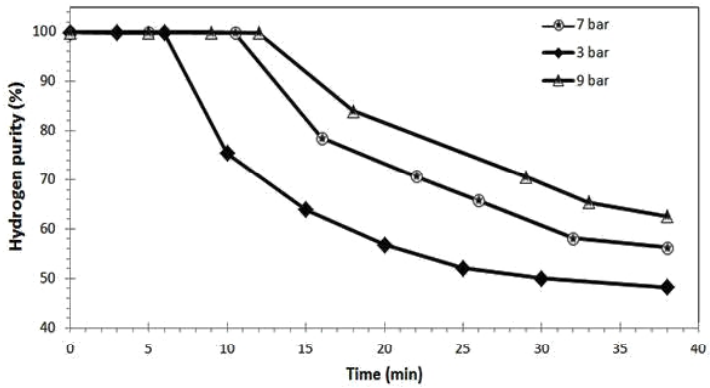

Fig.3. Effect of adsorption pressure on breakthrough curves at constant feed flow rate, 0.1 SLPM, for H_2/CO_2 mixture.

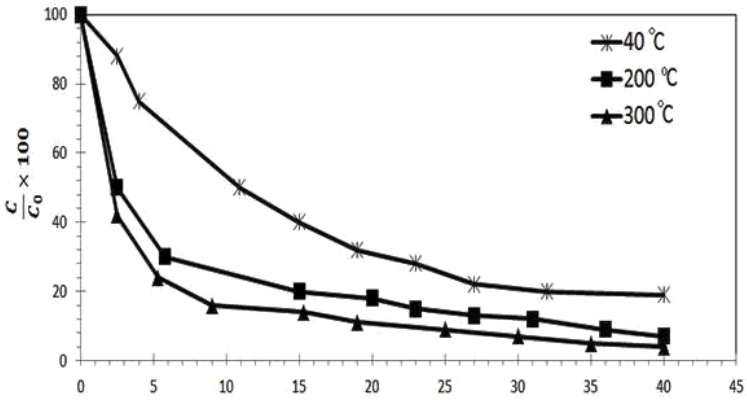

Fig.4. Desorption of CO_2 with pure hydrogen as purge gas at various regeneration temperature.

Fig. 4 shows the effect of purge gas temperature on desorption time of carbon dioxide from an adsorption bed saturated with 50% CO_2 in H_2 at 7 bar. In this figure, the change of carbon dioxide concentration to its initial concentration ($\frac{C}{C_0}$), desorbed from the bed, is plotted versus the desorption time at 40, 200 and 300 °C purging gas temperatures. 0.1 SLPM pure hydrogen was used as the purge gas. As illustrated in the figure, the desorption rate of carbon dioxide in 40 °C is slow and it increases as the temperature of the hydrogen increases. CO_2 concentration decreases immediately with the introduction of the purge gas at 200 °C. As illustrated in the figure, there is almost most no difference between 200 °C and 300 °C for bed regeneration time. Since, a separation process should be even more energy efficient, the upper limit of desorption temperature was selected about 250 °C, because a lower desorption temperature leads to lower energy requirement.

4.2.Experimental design

Using the CCD for modeling and optimization of the TPSA process, the range of three effective

parameters were determined by preliminary experiments and literature review. The levels of these variables are the different values at which the experiments must be performed. In this case, three independent variables were investigated at five levels. Adsorption time (Ad.t) was studied between 5-15 minutes, $\frac{P}{F}$ ratio was selected between 0.1-0.3 and regeneration temperature was selected between 30-250°C. The range of variables and their levels are presented in Table 2. A cyclic steady state condition was generally reached after 10 cycles. Thus for each experimental run, the adsorbent was exposed to 15 consecutive adsorption-desorption cycles. All experiments were performed with the following time distribution: step II: as much as designed by CCD. Step III: 2.5 min, step (IV and V): 2.5 min. The responses or dependent variables were measured during the experiments. Herein, targeted response variables were the hydrogen recovery, hydrogen purity and productivity. The ratio, productivity and recovery of the TPSA process was evaluated via equations 2, 3, and 4 [25].

$$\frac{\text{Purge}(P)}{\text{Feed}(F)} = \frac{\text{amount of hydrogen used in PG step}}{\text{amount of hydrogen inlet in AD step}} \quad (2)$$

Table 2. The range and levels of the independent variables

Variables	Range and level				
	-α*	-1	0	+1	+α*
$\frac{P}{F}$	0.1	0.129	0.2	0.27	0.3
Adsorption time	5	6.46	10	13.53	15
Regeneration temperature	30	74	140	205	250

α*: The distance of the axial points from the center point

Table 3. The designed experiments by CCD methodology and corresponding responses for the PSA process

Runs	The factors			Responses		
	$\frac{P}{F}$	Adsorption time (min)	Regeneration temperature	Purity (%)	Recovery (%)	Productivity $\frac{L}{s.gr}$
1	0.21	10.00	139.66	94.27	51.3519	1.27E-05
2	0.15	13.00	205.27	95.92	62.2444	1.63E-05
3	0.21	4.95	139.66	99.78	40.807	1.01E-05
4	0.26	13.00	205.27	96.07	53.986	1.43E-05
5	0.21	10.00	139.66	94.32	51.3694	1.27E-05
6	0.21	10.00	250	98.85	54.9859	1.47E-05
7	0.15	13.00	74.05	68.26	52.6632	1.10E-05
8	0.3	10.00	139.66	92.69	46.2924	1.19E-05
9	0.21	15.00	139.66	80.53	54.6057	1.29E-05
10	0.21	10.00	139.66	94.27	51.3497	1.27E-05
11	0.11	10.00	139.66	87.22	58.6525	1.44E-05
12	0.21	10.00	29.32	73.52	45.1783	9.93E-06
13	0.21	10.00	139.66	94.2	51.3244	1.27E-05
14	0.21	10.00	139.66	94.24	51.3378	1.27E-05
15	0.26	7.00	74.05	83.51	39.7857	9.37E-06
16	0.21	10.00	139.66	94.32	51.369	1.27E-05
17	0.26	7.00	205.27	99.85	45.8994	1.20E-05
18	0.15	7.00	205.27	94.84	51.5268	1.32E-05
19	0.26	13.00	74.05	76.62	45.2319	1.01E-05
20	0.15	7.00	74.05	84.87	47.8839	1.14E-05

(3)

$$\text{Recovery} = \frac{(\text{product eluted from AD step} - \text{product used in PG step}) \times \text{product purity}}{\text{feed from PR and AD step} \times \text{composition of Hydrogen in feed}}$$

(4)

$$\text{productivity} = \frac{H_2(L)\text{from AD step} - H_2(L)\text{used in PG step}}{\text{total cycle time}(s) \times \text{adsorbent used}(g)}$$

Twenty testswith different operating conditions, based on the CCD methodology, were designed and are presented in Table 3.

The tests were performed and the following second-order polynomial equations were obtained. Regression analysis showed that the data can be modeled by the following second order polynomial equations:

$$\text{Purity} = 46.98 + 262.08\frac{P}{F} + 3.94\times10^{-1}\text{Ad.t} + 1.92\times10^{-1}\text{T} + 1.33\times10^{-1}(\text{Ad.t})(\text{T}) - 7.10\times10^{-4}(\text{T})^2 - 569.82(\frac{P}{F})^2 - 1.85\times10^{-1}(\text{Ad.t})^2 \quad (5)$$

$$\text{Productivity} = 8.30 - 1.39\times10^{-5}\frac{P}{F} + 8.34\times10^{-7}\text{Ad.t} + 3.24\times10^{-9}\text{T} - 5.16\times10^{-8}(\text{Ad.t})^2 + 3.24\times10^{-9}(\text{Ad.t})(\text{T}) - 3.94\times10^{-11}\text{T}^2 \quad (6)$$

$$\text{Recovery} = 41.46 - 117.52\frac{P}{F} + 3.43\text{Ad.t} + 2.63\times10^{-2}\text{T} + 5.45\times10^{-3}(\text{Ad.t})(\text{T}) + 123.64(\frac{P}{F})^2 - 1.46\times10^{-1}(\text{Ad.t})^2 - 1.09\times10^{-4}\text{T}^2 \quad (7)$$

where, hydrogen purity, recovery and productivity are the response values and the terms are in the actual factor. Predicted models show an interaction between Ad.t and TR in the range that the experiments were performed. The analysis of variance (ANOVA) for the response quadratic model was investigated, so that values of "Prob > F" (p-value) less than 0.05 indicate the model terms are significant and values greater than 0.10 indicate they are not significant. The insignificant terms in the models were omitted and the analysis of variance was done again for the obtained reduced quadratic models and results are shown in Tables 4. F-value and p-value of the models imply that the acquired models are significant and acceptably predict the responses . "Pred R-Squared" represents the accuracy of the model to predict a response value. In this work, the "Pred R-Squared" for hydrogen purity was 0.8417 and was in reasonable agreement with the "Adj R-Squared" of 0.9379. The "Pred R-Squared" for hydrogen recovery and productivity were 0.9716 and 0.9380 and they were in reasonable agreement with the "Adj R-Squared" of 0.9886 and 0.9722, respectively. "Adeq Precision" measures the signal to noise ratio and a ratio greater than 4 is desirable. For hydrogen purity, hydrogen recovery, and productivity models this ratio was 20.247, 57.98, and 36.39, respectively. This value indicates an adequate signal. The overall performance of the model is expressed by "R^2", and the degree of correlation between the observed and predicted values is expressed by "Adj. R^2" [26]. The R^2 for hydrogen purity, recovery, and productivity models, were 0.9608, 0.9928, 0.9810 and the Adj.R^2 were 0.9379, 0.9886, and 0.9722, respectively, which suggests that the models are suitable for process behavior prediction in the design space.

4.3. Study on the effect of operational factors and the process optimization

Based on the reduced models, effect of the operating factors on the TPSA process was investigated using three dimensional surface graphs. The effect of regeneration temperature, adsorption time, and $\frac{P}{F}$ ratio on the hydrogen purity, recovery, and productivity are presented in Figs. 5, 6, and 7, respectively. In these 3D graphs the effect of two parameters are surveyed, whereas the other one is maintained constant. Effect of the adsorption time and $\frac{P}{F}$ ratio on hydrogen purity has been presented in Fig. 5a. It demonstrates that the hydrogen purity at constant regeneration temperature decreased as the adsorption time increased. This is due to the aggregation of carbon dioxide on the adsorbent, because when adsorption time increases the greater part of the bed becomes saturated with carbon dioxide and the purity of the outlet hydrogen decreases at a

Table 4. Analysis of variance the reduced quadratic model for A: hydrogen purity B: hydrogen recovery C: hydrogen productivity

Response	Source	Sum of squares	d_f	Mean square	F-value	p-Value Prob > F
A	Model	1510.22	7	215.75	41.99	< 0.0001
	A – (P/F)	33.44	1	33.44	6.51	0.0254
	B- (Ad.t)	251.25	1	251.25	48.9	< 0.0001
	C - (T)	985.52	1	985.52	191.81	< 0.0001
	BC	54.14	1	54.14	10.54	0.007
	A^2	42.82	1	42.82	8.33	0.0137
	B^2	39.38	1	39.38	7.66	0.017
	C^2	134.63	1	134.63	26.2	0.0003
	Residual	61.65	12	5.14		
	Lack of Fit	61.64	7	8.81	3939.5	< 0.0001
	Pure Error	0.011	5	2.24E-03		
	Cor Total	1571.87	19			
B	Model	569.77	7	81.40	236.09	< 0.0001
	A – (P/F)	184.54	1	184.54	535.27	< 0.0001
	B- (Ad.t)	199.79	1	199.80	579.51	< 0.0001
	C-(T)	145.56	1	145.56	422.20	< 0.0001
	BC	9.20	1	9.20	26.68	0.0002
	A^2	2.02	1	2.02	5.85	0.0324
	B^2	24.77	1	24.77	71.85	< 0.0001
	C^2	3.20	1	3.20	9.28	0.0102
	Residual	4.14	12	0.34		
	Lack of Fit	4.14	7	0.59	1916.13	< 0.0001
	Pure Error	0.00154	5	0.000308		
	Cor Total	573.91	19			
C	Model	5.82E-11	6	9.69E-12	111.81	< 0.0001
	A – (P/F)	8.00E-12	1	8.00E-12	92.33	< 0.0001
	B- (Ad.t)	7.91E-12	1	7.91E-12	91.21	< 0.0001
	C-(T)	3.56E-11	1	3.56E-11	410.82	< 0.0001
	BC	3.25E-12	1	3.25E-12	37.49	< 0.0001
	B^2	3.14E-12	1	3.14E-12	36.25	< 0.0001
	C^2	4.19E-13	1	4.19E-13	4.84	0.0466
	Residual	1.13E-12	13	8.67E-14		
	Lack of Fit	1.13E-12	8	1.41E-13	1760.97	< 0.0001
	Pure Error	4.00E-16	5	8.00E-17		
	Cor Total	5.93E-11	19			

constant value of $\frac{P}{F}$ ratio. As shown in the figure, a higher $\frac{P}{F}$ ratio results in higher hydrogen purity. Since when the $\frac{P}{F}$ ratio increases more of the high pure hydrogen is used to regenerate the bed. The combined effects of regeneration temperature and $\frac{P}{F}$ ratio at constant adsorption time have been shown in Fig. 5b. As can be seen in the figure, hydrogen purity increases drastically as the regeneration temperature increases and increases slightly as the $\frac{P}{F}$ ratio increases. This is due to the strong interaction between carbon dioxide and zeolite in the adsorption process. So, desorption of carbon dioxide did not take place efficiently at ambient temperature. Hydrogen purity increases as both of these parameters increase, but as shown

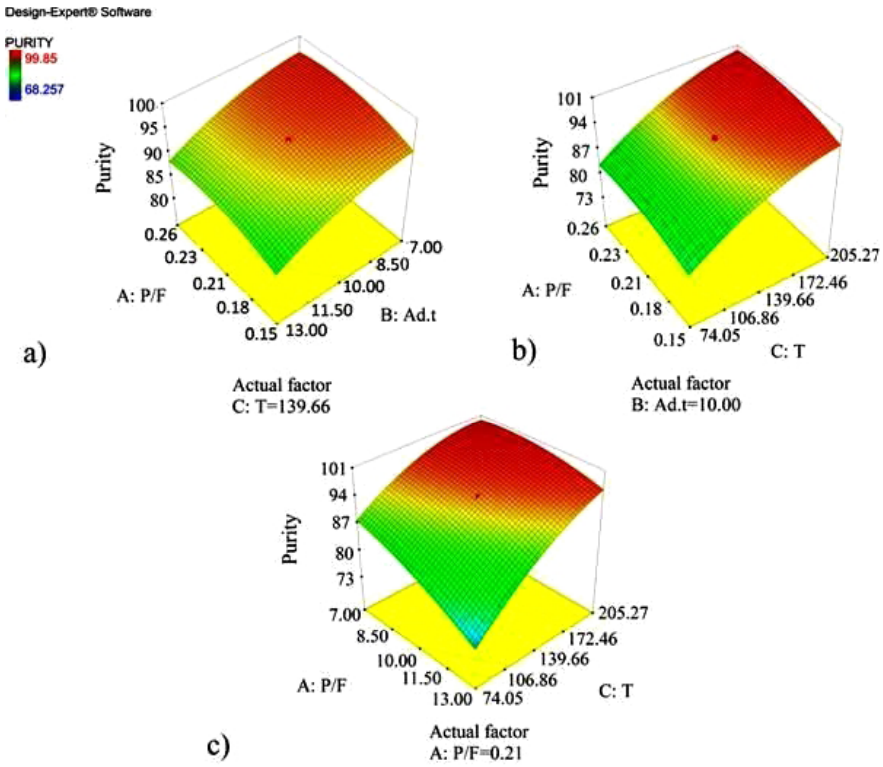

Fig. 5. Response surface graph of the hydrogen purity in the TPSA process as a function of a) P/F ratio and adsorption time b) P/F ratio and regeneration temperature c) adsorption time and regeneration temperature.

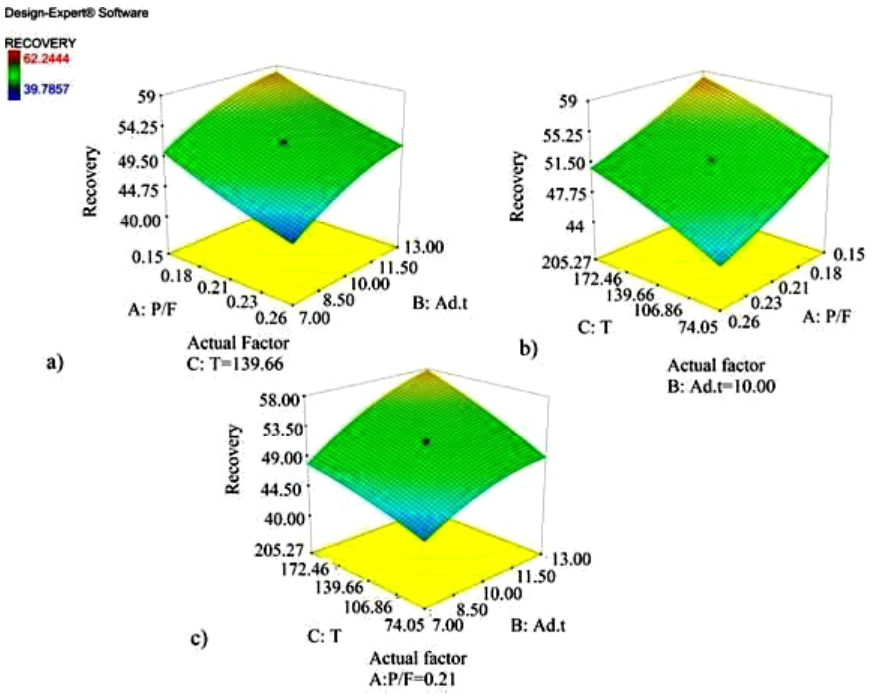

Fig. 6. Response surface graph of the hydrogen recovery in the TPSA process as a function of a) P/F ratio and adsorption time b) P/F ratio and regeneration temperature c) adsorption time and regeneration temperature

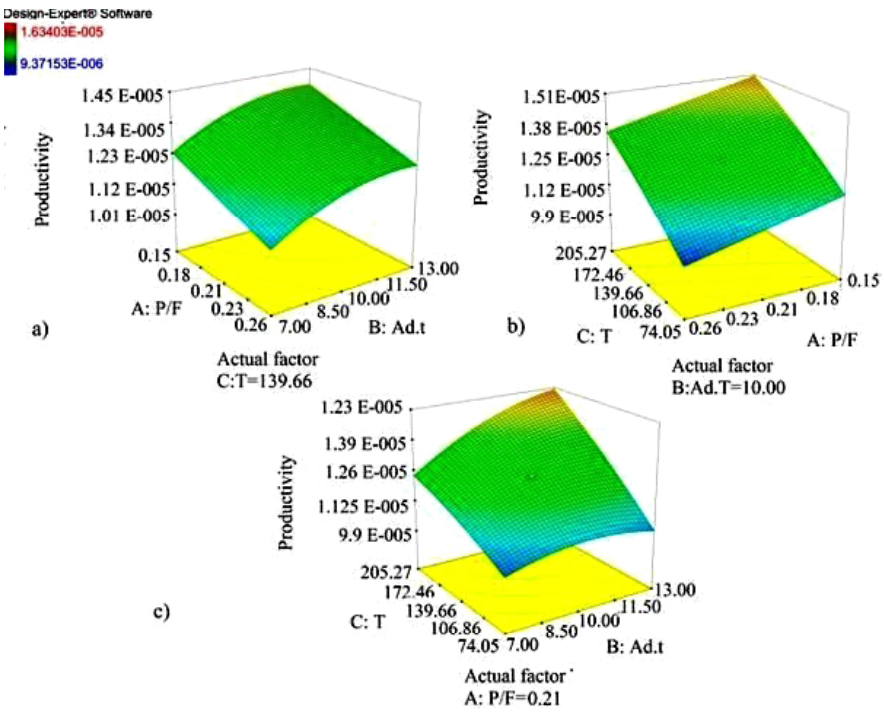

Fig. 7. Response surface graph of the hydrogen productivity in the TPSA process as a function of a) P/F ratio and adsorption time b) P/F ratio and regeneration temperature c) adsorption time and regeneration temperature

in the figure, at the high regeneration temperatures after about 0.21 of $\frac{P}{F}$ ratio the hydrogen purity is almost constant. This phenomenon illustrates that at a high regeneration temperature an almost appropriate regeneration of the bed occurs at about 0.21 of $\frac{P}{F}$ ratio and there is no need for higher hydrogen to purge the bed. In Fig. 5c the effect of adsorption time and regeneration temperature, at constant $\frac{P}{F}$ ratio, simultaneously demonstrate the hydrogen purity. This figure shows that hydrogen purity increases as regeneration temperature increases and decreases as the adsorption time increases. As shown in the figure, hydrogen purity decreases drastically with an increase in adsorption time at low regeneration temperature, and it slightly decreased with an increase of adsorption time at higher regeneration temperature. In other words, there is an interaction between regeneration temperature and adsorption time. When adsorption time increases, greater parts of the bed will be saturated by carbon dioxide; therefore, hydrogen purity will considerably decrease if complete regeneration of the bed doesn't occur. An almost complete desorption of carbon dioxide from the zeolite takes place at high regeneration temperature, and high pure hydrogen can be produced even in high adsorption times. These results are in good agreement with the literature.

Figure 6 shows the effect of operational factors on hydrogen recovery. As shown in Figure 6a, hydrogen recovery increases as the adsorption time increases and decreases as the $\frac{P}{F}$ ratio increases. The effect of regeneration temperature and $\frac{P}{F}$ ratio on hydrogen recovery is demonstrated in Figure 6b. As shown in the figure, hydrogen recovery increases as the regeneration temperature increase and decreases as the $\frac{P}{F}$ ratio increases. This is due to an increment in hydrogen purity that results in an increment of hydrogen recovery (equation (3)). Figure 6c shows the effect of regeneration temperature and adsorption time at constant $\frac{P}{F}$ ratio on hydrogen recovery. As shown in the figure, hydrogen recovery increases as the adsorption time and regeneration temperature increase. Increasing the adsorption time produces more hydrogen (as a product in step II) and this results in an increment in hydrogen recovery.

Figure 7 shows the effect of operational factors on

hydrogen productivity. As shown in the figure, the change in productivity is slightly similar to changes in recovery. Fig. 7a shows the effect of $\frac{P}{F}$ ratio and adsorption time at constant regeneration temperature on hydrogen productivity. The 3D graph shows that hydrogen recovery increased as the adsorption time increases and the P/F ratio decreases. In Fig. 7b the effect of regeneration time and $\frac{P}{F}$ ratio at constant adsorption time has been demonstrated. As shown in the figure, hydrogen recovery increases as the regeneration temperature oncreases and the $\frac{P}{F}$ ratio decreases. Fig. 7c shows the effect of adsorption time and regeneration temperature on hydrogen recovery. As shown in the figure, productivity increases as the adsorption time and regeneration temperature increase but this increment isn't linear at different regeneration temperatures, as it increases drastically at high regeneration temperature. This is due to increment in hydrogen purity at high regeneration temperature. These results are in good agreement with the literature.

4.4.Optimization of the operating factors

In this study, optimization of the process means finding the value of the operating factors to reach a desired point of response based on the proposed reduced RSM model. The optimization was performed using the related numerical facilities of the applied software.

To optimize the operating factors, the goals of operating factors (T_R, $\frac{P}{F}$ ratio, and Ad.t) were set "in range". Also, the desired goals for the hydrogen purity, recovery, and productivity responses were set at "maximized" or "in range". Seven states for different response values are compared in Table 5. In this table, the optimum values for operating factors have been predicted based on the goal of the responses. Generally, the optimum condition is selected based on the need of industries. The performance of hydrogen separation process depends on hydrogen purity, recovery, and productivity. The energy requirement for the process is usually proportional to the recovery, and size of the adsorbent bed is inversely proportional to the productivity. The maximum possible value of the hydrogen purity is often the most desirable case for hydrogen purification process in industry. Therefore, run 7 in Table 5 can be proposed as the most appropriate condition due to its highest hydrogen purity (99.88 %) and highest CO_2 capture. Confirmatory experiments were performed to evaluate accuracy and validate model prediction. The practically obtained results are also shown Table 5. As shown in the table, practical values are reasonably close to predicted values; therefore, the experimental data confirmed the accuracy of the models as well.

5. Conclusion

This research has studied the TPSA process of bulk separation of hydrogen and carbon dioxide utilizinglocal zeolite 5A as the adsorbent. The most outstanding findings of this work can be briefly stated as follows:

Table 5. Numerical optimization of the PSA process

No.	Productivity			Purity (%)			Recovery (%)			$\frac{P}{F}$	T (°C)	Ad.t (min)	Des
	G	Pre×10^5	Prac×10^5	G	Pre	Prac	G	Pre	Prac				
1	M	1.59	1.59	In	93.10	91.89	In	61.78	61.63	0.15	205.00	13.00	0.948
2	M	1.54	1.58	M	96.52	95.85	In	58.99	59.84	0.17	205.00	11.90	0.881
3	M	1.59	1.63	M	93.40	94.23	M	61.64	62.11	0.15	205.00	12.82	0.901
4	M	1.59	1.56	In	93.11	90.49	M	61.78	61.19	0.15	205.00	13.00	0.963
5	In	1.57	1.62	M	94.56	95.64	M	60.90	61.44	0.15	205.00	12.00	0.885
6	In	1.59	1.56	In	93.21	90.68	M	61.78	61.17	0.15	205.00	12.94	0.977
7	In	1.32	1.38	M	99.88	99.92	In	50.71	52.10	0.20	204.00	7.99	1.00

M: maximized, Pre: predicted value, Prac: practical value, Des: desirability, G: goal

(I): TPSA process for CO_2 capture from hydrogen was modeled and optimized properly using response surface methodology.
(II): Appropriate amount of operational factors, namely feed flow rate and adsorption pressure, were evaluated at 0.1 SLPM and 7 bar in the cyclic TPSA process, respectively.
(III): An appropriate upper limit of regeneration temperature of about 250°C as selected for experiments design based on re eneration experiments.
(IV): The effects of three important operational parameters including $\frac{P}{F}$ ratio, adsorption time, and regeneration temperature on hydrogen purity, recovery and productivity were evaluated by second order polynomial models.
(V): 3D graphs showed that hydrogen purity increased as the regeneration temperatures increased till about 205 °C, even at high adsorption time and low $\frac{P}{F}$ ratios.
(VI): Optimum conditions were proposed by RSM for maximum removal of CO_2, maximum hydrogen recovery and productivity in the TPSA process.
(VII): Since hydrogen purity is the most important factor for almost all hydrogen end-users, the best optimum condition was proposed based on maximum hydrogen purity. Maximum hydrogen purity (99.88 %) was predicted at T_R= 204°C, Ad.t= 7.99 min, and $\frac{P}{F}$= 0.2.
(VII): Validation of polynomial models for hydrogen purity, recovery, and productivity were performed by confirmatory tests. Experimental results confirmed the efficiency of the obtained models.

Nomenclature

Ad.t	adsorption time
$\frac{P}{F}$	Purge to feed ratio
T_R	Regeneration temperature
N	number of required tests
k	number of factors
N_0	number of same tests
Des	desirability
PSA	Pressure Swing Adsorption
RSM	Response Surface Methodology
TPSA	Thermal pressure swing adsorption

References

[1] Song C. “Global challenges and strategies for control, conversion and utilization of CO_2 for sustainable development involving energy, catalysis, adsorption and chemical processing”. Catal. Today. 2006, 115:2.

[2] Metz B., Davidson O., Coninck H., Loos M., Meyer L., “Carbon dioxide capture and storage, International Panel on Climate Control (IPCC)”. Cambridge University Press Cambridge; 2005.

[3] Di Sarli V., Di Benedetto A., “Laminar burning velocity of hydrogen–methane/air premixed flames”. Int. J. Hydrogen Energy. 2007, 32: 637.

[4] El-Ghafour S., El-Dein A., Aref A., “Combustion characteristics of natural gas–hydrogen hybrid fuel turbulent diffusion flame”. Int. J. Hydrogen Energy, 2010, 35: 2556.

[5] Ruthven D.M., “Principles of adsorption and adsorption processes”. John Wiley & Sons, 1984.

[6] Sircar S., Waldron W., Rao M, Anand M., “Hydrogen production by hybrid SMR–PSA–SSF membrane system”. Sep. Purif. Technol. 1999, 17: 11.

[7] Bastos-Neto M., Moeller A., Staudt R., Böhm J., Gläser R., “Dynamic bed measurements of CO adsorption on microporous adsorbents at high pressures for hydrogen purification processes”. Sep. Purif. Technol. 2011, 77:251.

[8] Manovic V., Anthony EJ., “Lime-based sorbents for high-temperature CO_2 capture—a review of sorbent modification methods”. Int. j. Environ. Res. and public health. 2010, 7: 3129.

[9] Hart A., Gnanendran N., “Cryogenic CO_2 capture in

natural gas". Energy Procedia. 2009, 1:697.

[10] Hauchhum L., Mahanta P., "Carbon dioxide adsorption on zeolites and activated carbon by pressure swing adsorption in a fixed bed". Int. J. Energy Enviro. 2014, 5:349.

[11] Tlili N., Grévillot G., Vallières C., "Carbon dioxide capture and recovery by means of TSA and/or VSA". Int. J. Greenhouse Gas Control. 2009, 3:519.

[12] Siriwardane R.V., Shen M.S., Fisher E.P., Losch J., "Adsorption of CO_2 on zeolites at moderate temperatures". Energy & Fuels. 2005, 19:1153.

[13] Siriwardane R.V., Shen M.S., Fisher E.P., Poston J.A., "Adsorption of CO_2 on molecular sieves and activated carbon". Energy & Fuels. 2001, 15:279.

[14] García S., Gil M., Pis J., Rubiera F., Pevida C., "Cyclic operation of a fixed-bed pressure and temperature swing process for CO_2 capture: experimental and statistical analysis". Int. J. Greenhouse Gas Control. 2013, 12:35.

[15] Frey D.D., Engelhardt F., Greitzer E.M., "A role for" one-factor-at-a-time" experimentation in parameter design". Res. Eng. Des. 2003, 14:65.

[16] Dutta S., Bhattacharyya A., Ganguly A., Gupta S., Basu S., "Application of response surface methodology for preparation of low-cost adsorbent from citrus fruit peel and for removal of methylene blue". Desalination. 2011, 275:26.

[17] Shafeeyan M.S., Daud WMAW., Houshmand A., Arami-Niya A., "The application of response surface methodology to optimize the amination of activated carbon for the preparation of carbon dioxide adsorbents". Fuel. 2012, 94:465.

[18] García S., Gil M, Martín C., Pis J., Rubiera F., Pevida C., "Breakthrough adsorption study of a commercial activated carbon for pre-combustion CO_2 capture". Chemical Engineering Journal. 2011, 171:549.

[19] Serna-Guerrero R, Belmabkhout Y, Sayari A. "Modeling CO_2 adsorption on amine-functionalized mesoporous silica: 1. A semi-empirical equilibrium model". Chemical Engineering Journal. 2010, 161:173.

[20] Mulgundmath V., Tezel FH., "Optimisation of carbon dioxide recovery from flue gas in a TPSA system". Adsorption. 2010, 16:587.

[21] Box GE., Wilson K., "On the experimental attainment of optimum conditions". Journal of the Royal Statistical Society Series B (Methodological). 1951, 13:1.

[22] Whitcomb P.J., Anderson M.J., "RSM simplified: optimizing processes using response surface methods for design of experiments", CRC press, 2004.

[23] Myers R.H., Montgomery D.C., Anderson-Cook CM., "Response surface methodology: process and product optimization using designed experiments", John Wiley & Sons, 2016.

[24] Anderson MJ., Whitcomb PJ., "Design of experiments", Wiley Online Library, 2000.

[25] Moon D-K., Kim Y-H., Ahn H., Lee C-H., "Pressure Swing Adsorption Process for Recovering H2 from the Effluent Gas of a Melting Incinerator". Ind Eng Chem Res. 2014, 53:15447.

[26] Montgomery D.C., "Design and analysis of experiments", John Wiley & Sons, 2008.